Received: 24 February 2023 | Accepted: 6 August 2023

DOI: 10.1111/1462-2920.16485

RESEARCH ARTICLE

ENVIRONMENTAL MICROBIOLOGY Applied Microbiology International

# Icescape-scale metabolomics reveals cyanobacterial and topographic control of the core metabolism of the cryoconite ecosystem of an Arctic ice cap

**Jarishma K. Gokul**[1,2] | **Luis A. J. Mur**[1] | **Andrew J. Hodson**[3,4] | **Tristram D. L. Irvine-Fynn**[5] | **Aliyah R. Debbonaire**[1] | **Nozomu Takeuchi**[6] | **Arwyn Edwards**[1,7]

[1]Department of Life Sciences, Cledwyn Building, Aberystwyth University, Wales, UK

[2]Department of Plant and Soil Sciences, University of Pretoria, Pretoria, South Africa

[3]Department of Arctic Geology, University Centre in Svalbard (UNIS), Longyearbyen, Svalbard, Norway

[4]Department of Environmental Sciences, Western Norway University of Environmental Science, Sogndal, Norway

[5]Department of Geography and Earth Sciences, Aberystwyth University, Wales, UK

[6]Department of Earth Sciences, Graduate School of Science, Chiba University, Chiba, Japan

[7]Department of Arctic Biology, University Centre in Svalbard (UNIS), Longyearbyen, Svalbard, Norway

**Correspondence**
Jarishma K. Gokul and Arwyn Edwards, Department of Life Sciences, Cledwyn Building, Aberystwyth University, Aberystwyth, SY23 3DD Wales, UK.
Email: jarishma.gokul@up.ac.za and aye@aber.ac.uk

**Funding information**
Great Britain Sasakawa Foundation; Natural Environment Research Council, Grant/Award Numbers: NE/S001034/1, NE/V012991/1; Norges Forskningsråd, Grant/Award Number: 288402; South Africa National Research Foundation, Grant/Award Number: 84991

## Abstract

Glaciers host ecosystems comprised of biodiverse and active microbiota. Among glacial ecosystems, less is known about the ecology of ice caps since most studies focus on valley glaciers or ice sheet margins. Previously we detailed the microbiota of one such high Arctic ice cap, focusing on cryoconite as a microbe-mineral aggregate formed by cyanobacteria. Here, we employ metabolomics at the scale of an entire ice cap to reveal the major metabolic pathways prevailing in the cryoconite of Foxfonna, central Svalbard. We reveal how geophysical and biotic processes influence the metabolomes of its resident cryoconite microbiota. We observed differences in amino acid, fatty acid, and nucleotide synthesis across the cap reflecting the influence of ice topography and the cyanobacteria within cryoconite. Ice topography influences central carbohydrate metabolism and nitrogen assimilation, whereas bacterial community structure governs lipid, nucleotide, and carotenoid biosynthesis processes. The prominence of polyamine metabolism and nitrogen assimilation highlights the importance of recycling nitrogenous nutrients. To our knowledge, this study represents the first application of metabolomics across an entire ice mass, demonstrating its utility as a tool for revealing the fundamental metabolic processes essential for sustaining life in supraglacial ecosystems experiencing profound change due to Arctic climate change-driven mass loss.

## INTRODUCTION

Glaciers host diverse and abundant forms of microbial life (Anesio & Laybourn-Parry, 2012; Hodson et al., 2008). Prevailing extreme weather conditions and nutrient limitations typical for glaciers (Ren et al., 2019) influence the resource pool available to microbes for growth and metabolism (Cook, Edwards, Takeuchi, & Irvine-Fynn, 2016; Hodson, Boggild, et al., 2010). On glacial ice surfaces cryoconite holes are acknowledged as 'hotspots' of microbial diversity (Edwards, Mur, Girdwood, Anesio, Stibal, Rassner,

et al., 2014) and biogeochemical cycling on glacial surfaces (Sawstrom et al., 2002; Tranter et al., 2004). Cryoconite holes form as a result of melting induced by their albedo-reducing dark sediment (Langford et al., 2010). This sediment, or cryoconite, is characterised as a microbe-mineral aggregate (Cook, Edwards, Takeuchi, & Irvine-Fynn, 2016; Langford et al., 2010; Takeuchi, Kohshima, Goto-Azuma, & Koerner, 2001; Takeuchi, Kohshima, & Seko, 2001) sourced from aeolian processes, supraglacial entrainment (Takeuchi, 2002) and algae, cyanobacteria and bacteria that promote granule formation and aggregation (Hodson, Cameron, et al., 2010; Langford et al., 2010).

Determining a relationship between glacial microbial communities, their metabolism and interaction with neighbouring ecosystems requires understanding of the link between the physical constraints and biogeochemistry across scales within the landscape, which can be facilitated through multi-omics approaches (Edwards et al., 2020). Dome-shaped ice caps represent glacial ice masses unconstrained by their underlying topography, arbitrarily distinguished from continental-scale ice sheets by surface areas <50,000 $km^2$. They represent unique systems for the study of supraglacial microbial community development, for supraglacial biomass is deposited across all aspects of an ice mass flowing radially from its centre, rather than along the single axis of a valley glacier. Where plateau ice caps reside at high elevations, periods of active melt which support ample biological growth (Anesio & Laybourn-Parry, 2012) are both brief and variable in extent from 1 year to the next. This places profound constraints on the development of functional, active microbiomes across their surfaces. As a result of their smaller size, ice caps could also represent accessible analogues of ice sheets that may be studied in their entirety. We previously showed that localised physical and geographic constraints play a significant role on the composition of bacterial communities within cryoconite on a dome-shaped ice cap (Gokul et al., 2016). The environment itself is dominated by a core bacterial community whose predominant members are cyanobacteria, alongside a stable core community of heterotrophic generalist taxa of mostly actinobacteria (Gokul et al., 2016). Consequently, dome-shaped ice caps at high elevations in the high Arctic represent attractive model systems for the study of ab initio cryoconite community development and functionality across scales when compared with the expansive scope of the few studies to conduct ice sheet scale sampling (Cameron et al., 2015).

In this study, we apply non-targeted metabolomics to investigate the metabolic potential apparent on ice cap surfaces. In doing so, we sought to identify metabolic processes present, as well the drivers of metabolic function in cryoconite communities across a high Arctic ice cap. Within cryoconite, primary production and respiration are closely coupled (Anesio et al., 2009), underpinning close links between community structure and function as revealed by amplicon sequencing and metabolome profiling (Edwards, Mur, Girdwood, Anesio, Stibal, Rassner, Hell, et al., 2014). Within analogous habitats such as microbial mats, metabolic adaptations to carbon and nutrient limitations are evident, for example through scavenging and recycling pathways (Varin et al., 2010). Other adaptations to cold environments can include changes in fatty acid metabolism, for example through variations in lipid membrane composition (Edwards et al., 2020). Therefore, by observing the metabolome it may be possible to determine organism and community responses to varying biotic and abiotic states with a high degree of functional information (Bundy et al., 2009; Lankadurai et al., 2013).

## EXPERIMENTAL PROCEDURES

### Study site and sampling

Foxfonna (Figure 1) is an ice cap in central Svalbard, located at 78°08′ N, 16°07′ E with an area of ca. 4 $km^2$ and ice cover distributed between 725 m in the South and 810 m in the North (Gokul et al., 2016). The upward migration of ELAs in Svalbard by ~100 m over the last 50 years (Noël et al., 2020), coupled with Foxfonna's exposed convex topographic setting facilitating aeolian wind erosion of seasonal snow, has resulted in much of the ice cap lying in the percolation or superimposed ice zones (Müller, 1962), minimising any appreciable accumulation. Samples of cryoconite were collected on the 23 August 2011, in conditions where the late season presented the maximum exposure of glacier bare ice and its resident cryoconite debris. Samples were collected from 38 cryoconite sites distributed across four sectors arranged by aspect (G1–G4). Debris was aspirated aseptically into 15 mL tubes, stored on ice in the dark for immediate transport to −80°C storage and then −80°C transfer to the United Kingdom. The details of environmental parameter determination and digital elevation mapping are provided elsewhere (Gokul et al., 2016).

### Metabolite extraction

Metabolites were extracted from the cryoconite of all 38 sites on Foxfonna. One hundred milligrams of freeze-dried cryoconite were processed by bead beating in 1:2.5:1 chloroform:methanol:water (HPLC-grade, Fisher, Loughborough, UK) as described previously (Cook, Edwards, Bulling, et al., 2016). Extracts were centrifuged and 50 μL of the solvent resuspended in vials of 200 μL 70% methanol: water, before analysis

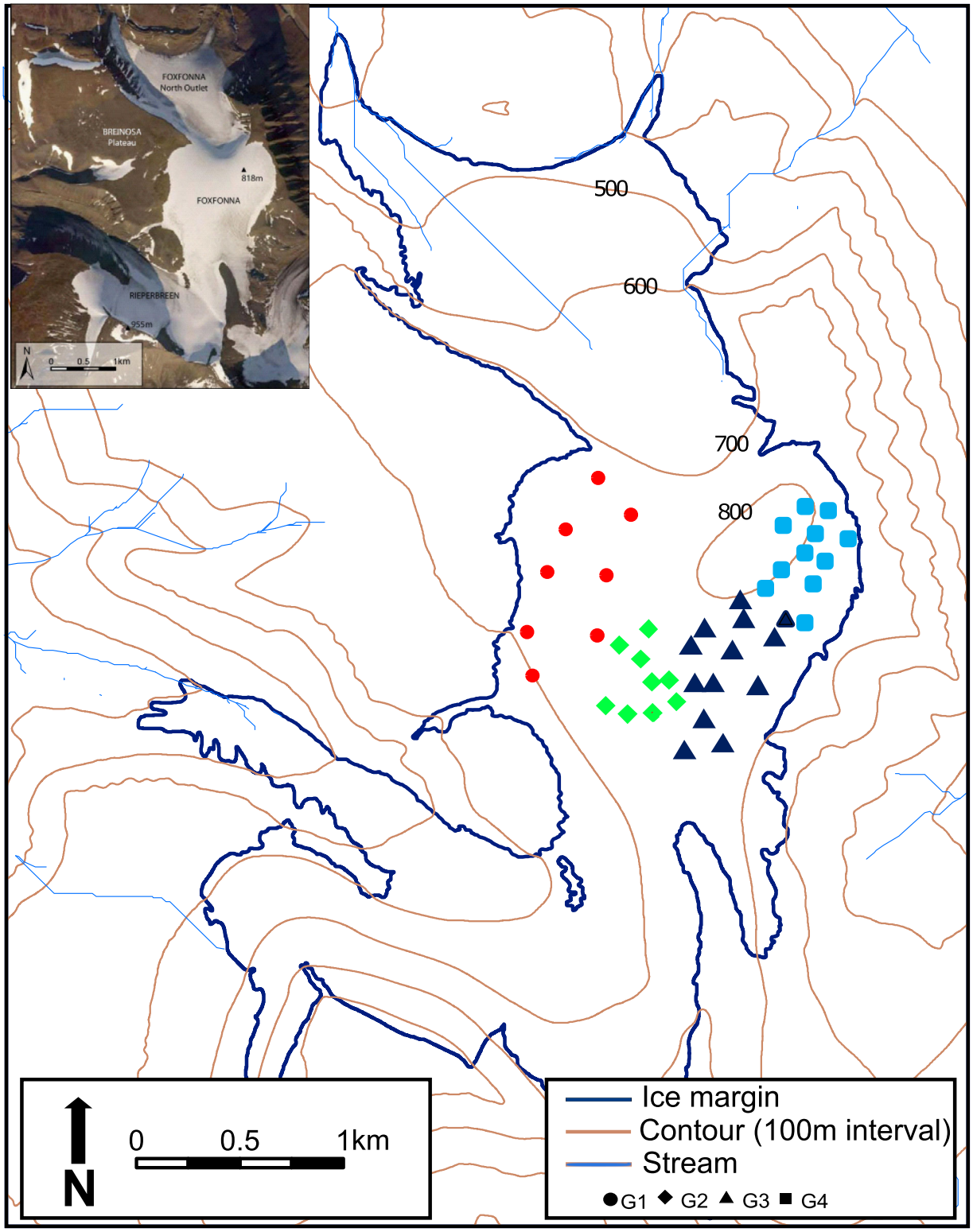


**FIGURE 1** Map of Foxfonna ice cap contour map showing the sampling points from sectors G1, G2, G3, and G4 across the ice cap surface.

on an LTQ linear ion trap (Thermo Electron Corporation). Data were acquired over the 100–1400 *m/z* range and processed in MATLAB (The MathWorks Inc.) for binning by unit mass and normalisation to percentage total ion count.

## Chemometric data analysis

Metabolite data was imported into PyChem (Jarvis et al., 2006) and observed using principal coordinates analysis (PCA; Edwards, Mur, Girdwood, Anesio,

Stibal, Rassner, Hell, et al., 2014) and PLSR. Models were cross-validated using full cross validation whereby data was split into a training set, a cross-validation set, and an independent test set. Metabolites of interest were extracted from the original dataset and further analysed in PRIMER 6/PERMANOVA + (PRIMER E) for multivariate statistical analysis and Metaboanalyst 3.0 (Zhu et al., 2015) for hierarchical cluster analysis. Metabolomes were examined against cartesian coordinates (Easting and Northing), dome geography, hydrology and cryoconite holes structure and chlorophyll *a* content to investigate environmental influence on the metabolome. Analysis of the taxa-metabolome relationship was also established by PLSR using OTU data from publicly available data (Gokul et al., 2016). Raw metabolite data are provided at: DOI: 10.5281/zenodo.7669756.

## RESULTS

Total metabolite extracts from 38 cryoconite samples, collected from the four sectors (G1, G2, G3, and G4) defined by aspect on Foxfonna (Figure 1), were subjected to non-targeted metabolite profiling using flow-injection electrospray-injection high-resolution mass spectrometry. The combined dataset generated 1398 discrete peaks. A remarkable, spatially-constrained ordination of the total metabolome was revealed via unsupervised chemometric analysis in the form of principal components analysis (PCA), discretely grouping sectors G1, G2, G3, and G4 on Foxfonna ice cap (Figure 2). Aspect affected the microbial metabolome most strongly, as significant sector effects were yielded from multivariate analysis using permutational multivariate analysis of variance (PERMANOVA) (*pseudo-F* = 4.5046, $p = 0.001$), supporting geographic influence on the metabolome through the influence of aspect. The presence of a sector-based effect in metabolite profile is further supported by analysis of similarity (ANOSIM, $R = 0.502$, $p = 0.001$).

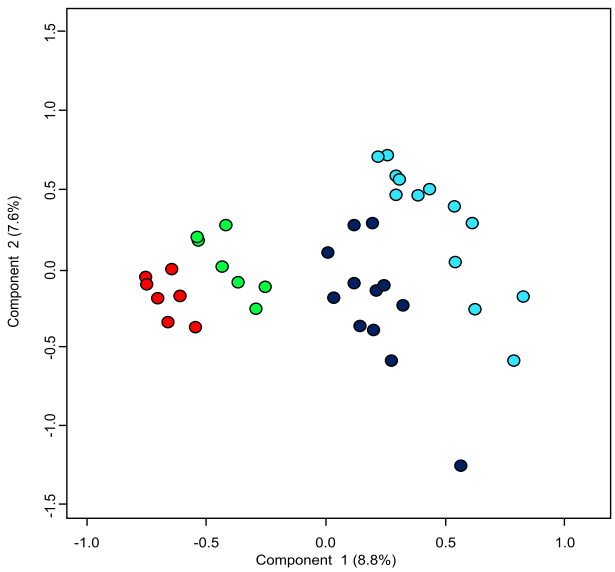


**FIGURE 2** PCA ordination of sites G1 (red), G2 (green), G3 (dark blue) and G4 (turquoise) showing a distinct level of disparity between each sector, correlating with geographical distribution.

## Variation in metabolite pathways across the ice cap

We sought to identify pathways associated with changes between sectors of the ice cap. Metabolites were tentatively identified by considering the multiple forms of ionization (including isotopes) for the metabolite as indicated on the DIMEdb database https://dimedb.ibers.aber.ac.uk/ (Accessed August 2016). Tentative identities were assigned for 70 metabolites. ANOVA *post-hoc* filtering of the metabolites (Bonferroni corrected for multiple comparisons) suggested the most prominent major sources of variation (Table 1). This indicated changes in the community cluster by sector and particularly between G1, and G2 with G3 and G4 (Figure 3A). These suggested changes in metabolites linked to were driven by major metabolites in nucleic acid biosynthesis (Figure 3B), for example, dihydroorotate, 5′-methylthioedenosine, the tricarboxylic acid (TCA) cycle (Figure 3C), for example, 2-oxobutanoate, nitrogen assimilation, polyamine (homoglutamine, N-acetylglutamic acid, GABA; Figure 3D), pentose phosphate pathway/photosynthesis (erythrose-4-phosphate) and lipid biosynthesis (Figure 3E) and photosynthesis (Figure 3F) Sn-glycerol-3-phosphate, stearic acid [C18:0]. To explore the importance of these pathways, their constituent metabolites were identified and extracted from the data matrix. Their variation between different sectors was examined by hierarchical cluster analysis (HCA).

## Exploring spatial variation in biochemical pathways

Examining nucleotide-associated metabolites by HCA with associated heat map to show the relative levels suggested a western (G1, G2)/eastern (G3, G4) split (Figure 3B). However, the within-sector variation was considerable, as also indicated by PCA analysis explaining only 27.8% of the metabolite variation in PCs 1 and 2 (Figure 4E) so specific differences were difficult to define. However, sector G3 generally had lower levels of adenine monophosphate (AMP), guanine monophosphate (GMP), phosphoribosyl pyrophosphate (PRPP), thymidine and 3′5-cyclic deoxyAMP (dAMP), while adenosine and inosine were higher in sector G4. Lower levels of allantoin, urate,

**TABLE 1** Major sources of variation as defined by post hoc ANOVA filtering, including tentative metabolite identification.

| Metabolite | *F* value | *p*-value | False discovery rate |
|---|---|---|---|
| 2-oxobutanoate | 78.421 | 1.32E-15 | 9.22E-14 |
| Ferulic acid | 41.021 | 1.49E-11 | 5.22E-10 |
| Homoglutamine | 23.211 | 1.89E-08 | 4.42E-07 |
| Gluconic acid | 19.898 | 1.06E-07 | 1.85E-06 |
| Syringic acid | 18.379 | 2.48E-07 | 3.47E-06 |
| Dihydroorotate | 16.847 | 6.10E-07 | 7.11E-06 |
| GABA | 15.715 | 1.22E-06 | 1.22E-05 |
| Erythrose-4-phosphate | 13.738 | 4.41E-06 | 3.86E-05 |
| Glucosaminic acid | 12.652 | 9.32E-06 | 7.25E-05 |
| 3-4-dihydroxy-L-phenylalanine | 11.485 | 2.16E-05 | 0.000151 |
| Maltose | 11.017 | 3.05E-05 | 0.000194 |
| R-S-lactoylglutathione | 10.87 | 3.41E-05 | 0.000199 |
| Riboflavin | 10.647 | 4.04E-05 | 0.000218 |
| Jasmonic acid | 10.259 | 5.44E-05 | 0.000272 |
| Tyrosine | 9.9445 | 6.96E-05 | 0.000312 |
| 2′,3′-cyclic GMP | 9.9115 | 7.14E-05 | 0.000312 |
| Adenosine | 9.3311 | 0.00011338 | 0.000467 |
| Stearic acid | 8.8992 | 0.00016121 | 0.000627 |
| Urate | 8.2515 | 0.00027684 | 0.00102 |
| Pelargonidin | 8.0696 | 0.00032316 | 0.001131 |
| N-acetyl-L-glutamate-5-phosphate | 7.8712 | 0.00038318 | 0.001277 |
| Naringenin | 7.7082 | 0.00044125 | 0.001404 |
| 5′-methylthioadenosine | 7.5222 | 0.00051901 | 0.00158 |
| O-acetyl-L-homoserine | 6.4453 | 0.0013671 | 0.003988 |
| Flavin mononucleotide | 6.1148 | 0.0018593 | 0.005204 |
| 3′,5′-cyclic dAMP | 6.0735 | 0.0019328 | 0.005204 |
| Docosahexaenoic acid | 6.0066 | 0.0020586 | 0.005337 |
| Fucoxanthin | 5.9402 | 0.0021916 | 0.005479 |
| Ribulose-5-phosphate | 5.8159 | 0.0024661 | 0.005953 |
| Linolenic acid | 5.4239 | 0.0035943 | 0.008387 |
| Catechin | 5.2454 | 0.0042773 | 0.009658 |
| Coniferyl aldehyde | 5.0501 | 0.0051831 | 0.011338 |
| Sn-glycerol-3-phosphate | 4.9979 | 0.0054578 | 0.011577 |
| Oxalacetate | 4.8692 | 0.0062024 | 0.01277 |
| Proline | 4.7431 | 0.0070366 | 0.014073 |
| Neoxanthin | 4.709 | 0.0072812 | 0.014158 |
| Myricetin | 4.662 | 0.0076339 | 0.014371 |
| Inosine | 4.6216 | 0.0079516 | 0.014371 |
| Cystathionine | 4.6147 | 0.0080067 | 0.014371 |
| Xanthosine-5′-phosphate | 4.5677 | 0.0083967 | 0.014694 |
| Adenine | 4.5263 | 0.0087567 | 0.01474 |
| Arachidonic acid | 4.5165 | 0.008844 | 0.01474 |
| Thymidine | 4.49 | 0.0090853 | 0.01479 |
| Fumarate | 4.4447 | 0.0095135 | 0.015135 |
| Citric acid | 4.2744 | 0.011323 | 0.017613 |
| ATP | 4.1627 | 0.012702 | 0.019328 |
| Kaempferol | 4.1223 | 0.013243 | 0.019724 |

(Continues)

TABLE 1 (Continued)

| Metabolite | *F* value | *p*-value | False discovery rate |
|---|---|---|---|
| Serine | 4.0452 | 0.014345 | 0.02092 |
| Cytosine | 3.8768 | 0.017096 | 0.024423 |
| Fructose-1,6-bisphosphate | 3.8261 | 0.01803 | 0.025241 |
| Spermine | 3.8005 | 0.01852 | 0.02542 |
| Oleic acid | 3.7741 | 0.01904 | 0.02563 |
| Cysteine | 3.6846 | 0.020924 | 0.027635 |
| Linoleic acid | 3.6591 | 0.021494 | 0.027862 |
| Pyrophosphate | 3.5952 | 0.022998 | 0.029271 |
| O-succinyl-L-homoserine | 3.5381 | 0.024436 | 0.030545 |
| Indole-3-glycerol-phosphate | 3.4821 | 0.025935 | 0.03185 |
| Glucosamine | 3.4454 | 0.02697 | 0.03244 |
| Hexose-phosphate | 3.4326 | 0.027342 | 0.03244 |
| Xanthoxin | 3.4049 | 0.028163 | 0.032856 |
| Antheraxanthin | 3.2694 | 0.032569 | 0.037374 |
| Palmitic acid | 3.2169 | 0.034463 | 0.03891 |
| Sphinganine-1-phosphate | 3.2 | 0.035097 | 0.038997 |
| Mannitol | 3.1788 | 0.035909 | 0.039231 |
| 2′,3′-cyclic AMP | 3.1655 | 0.036428 | 0.039231 |
| GTP | 3.1228 | 0.03815 | 0.040462 |
| Asparagine | 3.0828 | 0.039841 | 0.041617 |
| Alpha-carotene | 3.0693 | 0.040428 | 0.041617 |
| 5-HPETE | 3.0328 | 0.042063 | 0.042672 |
| Sinapaldehyde | 3.0163 | 0.042824 | 0.042824 |

hypoxanthine, adenine, xanthine, inosine monophosphate and adenosine diphosphate were observed in G3 compared to all other sectors.

The prominence of 2-oxobutanoate as a West–East discriminator in Figure 3B led us to explore the potential differences in the TCA cycle metabolites. For TCA cycle-associated intermediates, the first two principal components accounted for 71.7% of the variation in the observed TCA intermediate concentrations (Figure 4A). Comparing these variables by HCA and heat map, suggested some weak Western-Eastern clustering when all TCA metabolites were considered (Figure 3C). However, the levels of oxalacetate, oxoglutarate, 2-oxobutanoate and malate were higher in the western sectors (G1 and G2).

The cryoconite metabolome also showed that 73.6% of total variation observed was due to metabolites integral to polyamine synthesis (Figure 4B). Using the KEGG arginine and proline metabolism map (map00330), metabolites forming part of the nitrogen assimilation pathway leading to polyamines were targeted in the data matrices. Those that could be unambiguously identified included α-ketoglutaric acid which provides the carbon skeleton for amino acids, and the key assimilates glutamate and glutamate semialdehyde. The amino acids proline, and ornithine together with their intermediate 1- pyrroline-5-carboxylic acid (pyrolline-5C) as well as citrulline were identified. Gamma-aminobutyric acid (GABA), was also included as it can link glutamate and TCA cycle metabolism via the GABA-shunt which can contribute to α-ketoglutaric acid levels (Mahawar et al., 2022). Comparison of these metabolites by HCA and heatmap suggested no clear western-eastern split, although G1 samples (the most westerly) appeared to be distinctive. Thus, GABA, proline, and α-ketoglutaric acid were at lower levels in most G1 samples, compared to others (Figure 3D).

Another important component of primary metabolism involves lipids, and it was noted that lipid breakdown products were identified as notable sources of variation (Table 1), despite the lower observed variance of 56.6% explained by the first 2 PCs (Figure 4C). Comparing lipid-associated metabolites using a HCA and heat map suggested that samples from in the western sectors G3 and G4 clustered separately from those of eastern sectors G1 and G2, which were similar (Figure 3E). G4 was distinctive in having relatively lower levels in polyunsaturated derivatives of phospholipid acyl chains, linolenic acid (C18:2), linolenic acid (C18:3) and arachidonic acid (C20:4).

Given that nucleotide biosynthesis showed differences between western and eastern sectors

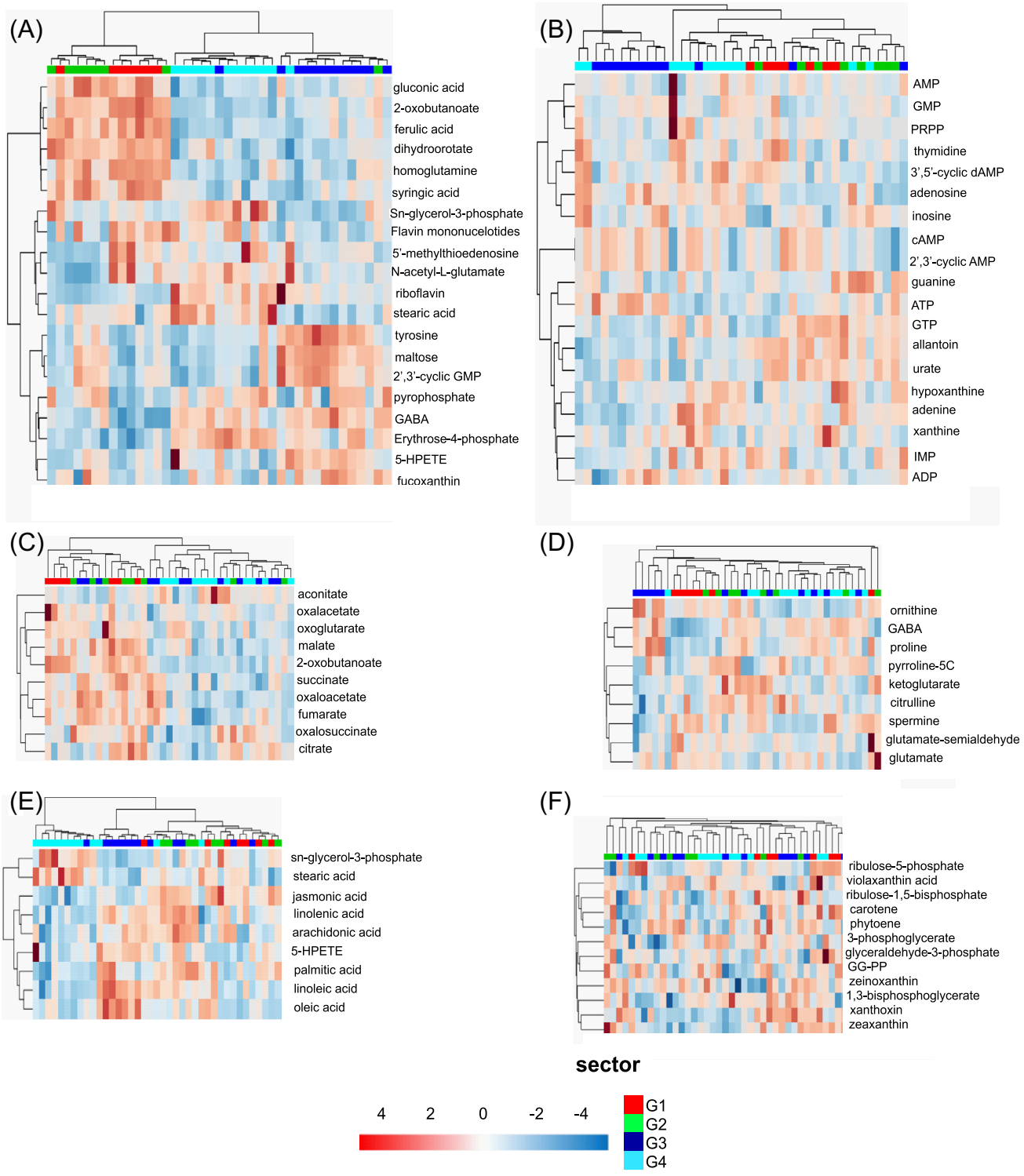


**FIGURE 3** Hierarchical cluster analysis of the major metabolic pathways in Foxfonna ice cap cryoconite communities. (A) Pathways of essential importance were identified as nucleic acid synthesis, TCA cycle, fatty acid synthesis and polyamine synthesis pathways. (B) Heatmap showing variable expression in nucleic acid synthesis activity with distinct clustering of sectors G1–G2 and G3–G4 (C) Heatmap showing TCA intermediates with high significant activity and clustering apparent in sectors G1 and G2. (D) Heatmap of polyamine synthesis depicting that sector G4 is distinguished by low activities when compared to the other three sectors. (E) Heatmap of lipid synthesis with clustering of high activity metabolites along sector G4. (F) Heatmap showing clustering in carotenoid synthesis apparent at G1.

(Figure 3B), which was partially reflected in some amide metabolism (Figure 3D), we also examined carbon fixation as a potential variable across the sectors. Identified photosynthesis associated metabolites showed no sector-specific accumulation patterns which implies the broad importance of photosynthesis in

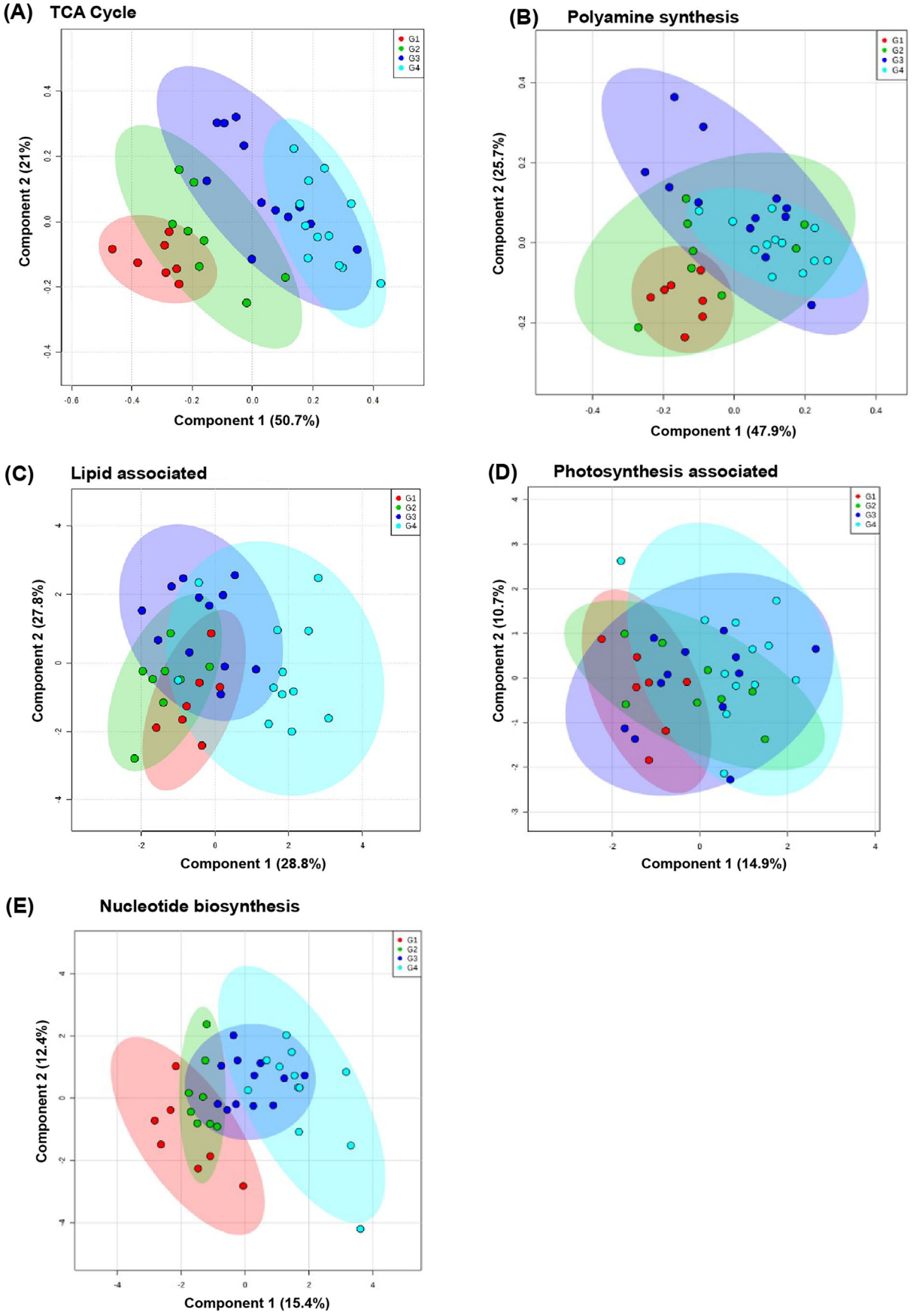


**FIGURE 4** Principal component analysis of metabolite profiles in the TCA cycle (A), polyamine synthesis (B), lipid biosynthesis (C), photosynthesis (D) and nucleotide biosynthesis (E). Sectors are coded as G1 (red), G2 (green), G3 (dark blue) and G4 (turquoise).

sustaining communities across the ice cap (Figures 3F, 4D).

## Interactions between the microbiome, environment, and metabolomes in Foxfonna cryoconite sectors

To understand the interaction between the physical environment, across ice cap metabolomes and the bacterial community of Foxfonna cryoconite, we used V1-V3 16S rRNA gene region profiles from the same samples, previously described (Gokul et al., 2016) and publicly available at EBI-SRA (SRP067436: PRJNA306097). A comparison of the Spearman rank value of these metabolites on the ice cap (Table 1) against the complementary operational taxonomic units (OTUs) with a relative abundance of above 0.1% (Table S1), displayed a weak, positive correlation ($R = 0.179$, $p = 0.04$) when analysed using the Mantel-based test RELATE.

Partial least squares regression (PLSR) modelling analysed the effects of sector, keystone taxa, core bacterial taxa with relative abundance >1% (Gokul et al., 2016) and environmental variables for geographic coordinates (Easting and Northing). Among the latter were: slope, aspect, curvature, hydrological indices (flow accumulation area, predicted meltwater discharge), incident radiation (energy and hours of exposure), positive degree days (PDD), chlorophyll content (Chl-A), and apparent cryoconite area, (Irvine-Fynn et al., 2010). The keystone and core OTU, denovo40205, identified as *Phormidesmis* sp. (Gokul et al., 2016) strongly adheres to the expected proportional fit exhibiting a robust correlation between predicted and actual regressions (Figure 5A). The metabolome predicted influences from incident radiation energy (IRR ($kW/m^2$), Figure 5B) and hours of exposure to sunlight (IRR hours, Figure 5C).

Analysis of the metabolites with core and keystone taxa as well as environmental parameters described in Gokul et al. (2016) by distance based redundancy ordination (dbRDA), displayed a clear and strong influence of parameters separating metabolites in the eastern sectors (G1 and G2) from the western sectors (G3 and G4) (Figure 6). The predictor variables that best explain 45.4% of total variation in metabolites have high positive and negative associations for Eastings, Northings and lower (yet significant) associations for the parameters aspect, PDD, Chl *a*, ACA, and taxa *Curvibacterium*-22,304, *Frigoribacterium*-32,521, *P. daechungensis*-61,341, *Phormidesmis*-40,205, *Novosphingobium*-11,564, *Rhizobium*-53,430, *Massilia*-5709, and *Eubacterium*-1447. The relative influence of biotic and abiotic factors as predictors of metabolite patterns were tested in the distance-based linear models where marginal tests reveal 11 out of 18 environmental parameters (pseudo-$F$ range = 2.3389–12.721, $p$ range = 0.001–0.043) and 7 out of 20 OTUs (pseudo-$F$ range = 2.9501–4.9933, $p$ range = 0.001–0.035) were significant contributors (Table S2). Sequential tests using $r$-squared selection revealed that the derived model was heavily influenced by geographic position (E, pseudo-$F = 12.721$, $p = 0.001$; N, pseudo-$F = 4.3482$, $p = 0.001$), PDDs (pseudo-$F = 3.6469$, $p = 0.008$) and chlorophyll a (pseudo-$F = 2.2088$, $p = 0.033$) (Table S3). Overall, the combined effects of these biotic and abiotic parameters have an integral role in shaping the cryoconite metabolome.

## DISCUSSION

Metabolomics-based characterisation of the interaction between organism and environment is an emerging 'omic approach that can provide great insight into the changes associated with climatic and biotic factors at the molecular level (Lankadurai et al., 2013). In the context of this study, we sought to traverse the metabolic icescape of Foxfonna, an ice cap in the high Arctic, to understand how the metabolomes of cryoconite habitats are governed by physical and microbial processes. While comparisons between different regions (Edwards, Mur, Girdwood, Anesio, Stibal, Rassner, et al., 2014), inventories of singular habitats (Lutz et al., 2015), and in situ experiments on the glacial surface (Cook, Edwards, Bulling, et al., 2016) have been conducted before, to our knowledge this is the first study to examine the metabolomic variation at the scale of an entire ice mass. Our study focuses on contemporaneous sampling across the entire ice mass at a time near the end of the summer season when bare ice is exposed. Necessarily, this is a single time point study, potentially integrating the development of the cryoconite communities to that point within the growing season. While other cryoconite within other regions of the Arctic shows stable community structure within the summer period (Gokul et al., 2019) future studies could address the question of whether temporal changes are reflected in supraglacial metabolomes at different timescales. Previously we have reported the bacterial community structure of the same cryoconite habitats distributed across Foxfonna (Gokul et al., 2016), facilitating comparison between microbiome and metabolome in the present study. The metabolomic profile presented here establishes significant influences at the biotic and abiotic levels upon fundamental biological pathways. This provides stronger insights into the active microbiota of Foxfonna's cryoconite, enhancing our understanding of community development, dynamics, and functionality required for successful microbial colonization of glacial ice surfaces at high elevation in the high Arctic.

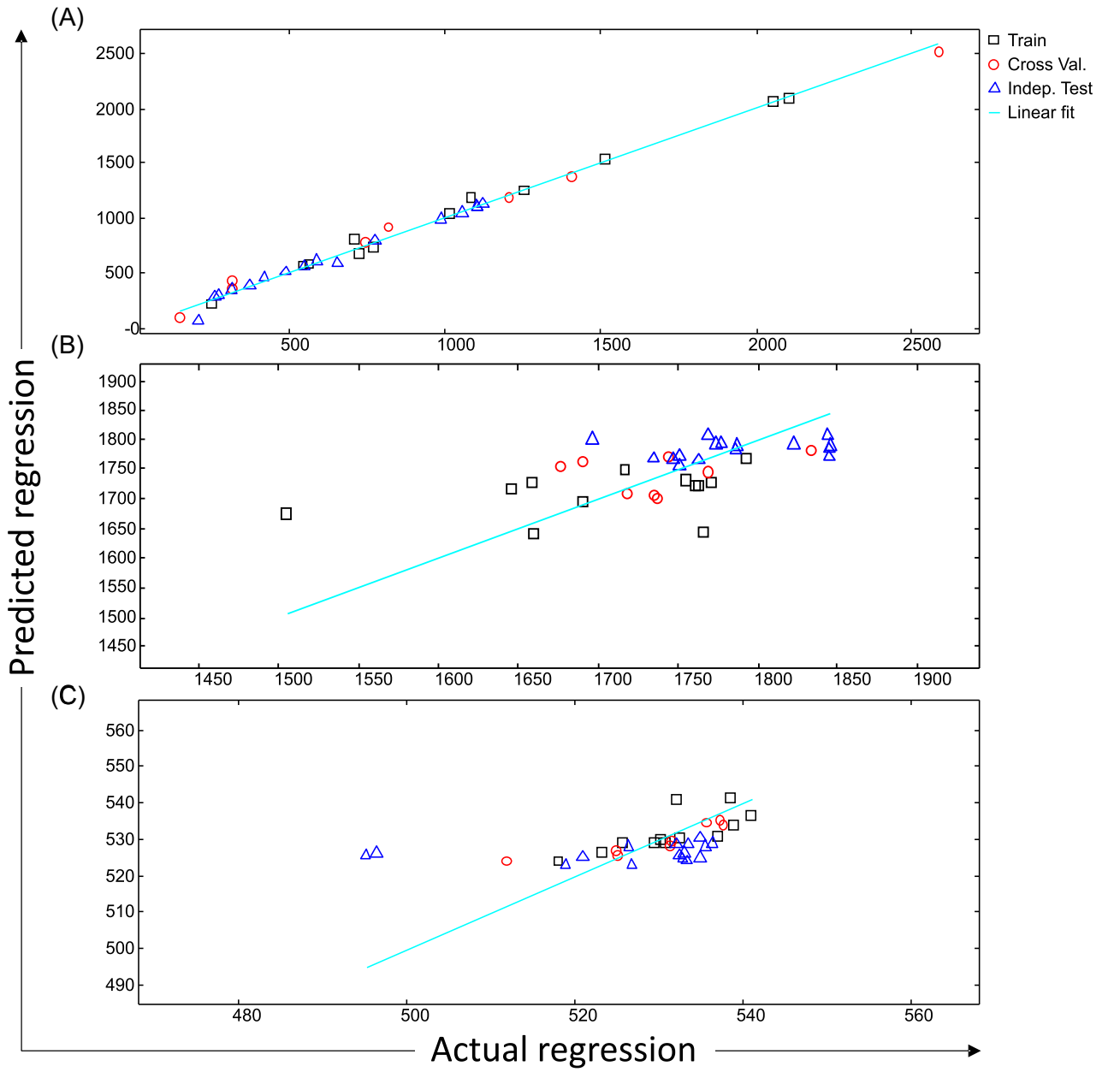


**FIGURE 5** PLS regression modelling of all metabolites on Foxfonna dome show that (A) the relative abundance of core taxon *Phormidesmis* denovo40205* fits the metabolite regression model best while Irradiation energy (kw; B), and period of irradiation (hours, C) show some influence, inferring their importance in shaping the cryoconite metabolome of the ice cap.

## Spatial variation in biosynthetic potential within cryoconite metabolomes

We found clear variation in the cryoconite community metabolomes according to sector on the surface of the ice cap by unsupervised and supervised methods (Figures 2–4) as well as multiple multivariate tests. Given the high-elevation dome shape of the ice cap, the metabolic profile of Foxfonna suggests a dynamic relationship between biosynthetic metabolites and ice mass topography. Biological proliferation as indicated by nucleotide synthesis essential for genome replication and gene transcription is abundant across the surface of the ice cap and is evidenced by the distribution of purine and pyrimidine metabolites across all the sectors with different intermediates accumulating in western and eastern sectors (Figure 3B).

A further indicator of biological activity is provided by the levels of TCA intermediates. These link bioenergetic metabolism with carbohydrate, amino acid and fatty acid degradation. A key intermediate in the TCA cycle is α-ketoglutarate, which is a crucial precursor metabolite for amino acid biosynthesis. This metabolite proved to be particularly abundant in the cryoconite

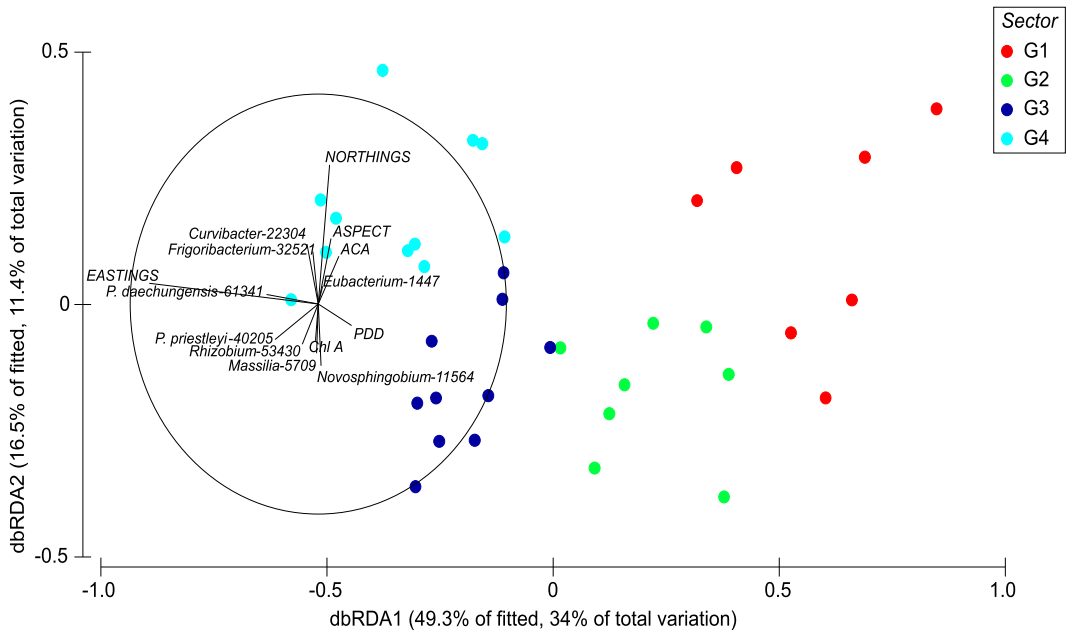


**FIGURE 6** Distance based redundancy ordination (dbRDA) of the combined variation in total Foxfonna ice cap metabolites highlighting the significant contributors from environmental and bacterial OTU parameters. Metabolites clearly separate into the different sectors on the dome shaped ice cap demonstrating geographical influence.

samples collected in the westerly sectors (G1 and G2) on Foxfonna (Figure 3C). A more focused examination of other TCA cycle intermediates also indicated a tendency for greater levels in sectors G1 and G2 (Figure 3C). This could indicate that TCA cycle activities and therefore ATP generation were more prominent in G1 and G2 and could be linked to higher levels of microbial activity.

## Central importance of photosynthetic carbon fixation via cyanobacteria

Interestingly, in our metabolomic assessment, identified photosynthesis-associated metabolites showed no clear trend of sector-specific accumulation patterns that could suggest a differential impact for solar irradiation (Figure 3F). We interpret this as evidence that photosynthetic carbon fixation is of central importance for community function throughout the study area. Autotrophs present on Foxfonna include photosynthesising algal species (*Chlamydomomas* and *Chloromonas*; Edwards et al., 2016), cyanobacteria (*Phormidesmis* and *Nostoc* species; Gokul et al., 2016) and photosynthetic bacteria (*Chloroflexi*) that can provide the organic carbon required by cryoconite communities (Murakami et al., 2022). The global metabolite regression model and high relative abundance of cyanobacteria across the ice cap, specifically the core taxon *Phormidesmis*-40,205 that corresponds with the widely acknowledged Arctic cryoconite ecosystem engineer *Phormidesmis priestleyi* (Edwards, Mur, Girdwood, Anesio, Stibal, Rassner, Hell, et al., 2014; Gokul et al., 2019; Hodson, Cameron, et al., 2010; Langford et al., 2010, 2014; Murakami et al., 2022; Segawa et al., 2017; Uetake et al., 2016), suggests that this cyanobacterial species may be essential to multiple metabolic process in ice cap cryoconite ecosystems. PLS regression will identify variables which correlate with a given features. Due to the multivariate nature of the correlations, different subsets of the data, that is, a training set, independent test, cross-validation are projected. A linear correlation based on the different sub-datasets (shown as between predictive and actual regression, Figure 5) shows that the derived correlation has robust statistical power. Using PLS regression, the overall metabolomic profile correlated significantly and positively with the relative abundance of *Phormidesmis*-40,205 indicating the inherent involvement of this organism in metabolism by cryoconite communities (Figure 5A). Relationships were also observed for parameters relating to solar energy receipt (Figure 5B, C) but to a lesser extent than the impact of *Phormidesmis*-40,205 relative abundance (Figure 5A). This is further reinforced by dbRDA (Figure 6) which draws out *Phormidesmis*-40,205 along with other biotic and abiotic factors in shaping the cryoconite metabolome. Combined, these observations speak to the importance of *Phormidesmis priestleyi* as a transducer of solar energy received by cryoconite communities on this high Arctic ice cap. Previous work on the metabolism of cryoconite on north-facing Arctic glaciers (Anesio et al., 2009) describes the correlation of primary production and respiration rates, whereas when taken together here, the distinctive spatial

patterns of photosynthesis and heterotrophic metabolism associated metabolites imply a potential decoupling to some extent.

The metabolome of *Phormidesmis*-dominated cryoconite holes subjected to experimental perturbation of solar radiation receipt in Greenland (Cook, Edwards, Bulling, et al., 2016) showed dramatic responses to light limitation, with concomitant upregulation of cyclic AMP, cyclic GMP and fucose catabolism, interpreted as mediating a phototactic response. Here, we observed clear trends in the abundance of the important signalling molecules cyclic AMP and cyclic GMP according to sector, with the greatest concentrations in eastern sectors G3 and G4, where lower concentrations of activity-related biomarkers were observed. While cAMP is a common second messenger, this may indicate that carbon fixation through cyanobacterial photosynthesis may be resilient to changes in the solar receipt across the ice cap through compensatory mechanisms within cryoconite cyanobacteria.

It was notable that the key fatty acids identified also showed a sectorial difference (Figure 3E) which appeared like that seen with the nucleotides (Figure 3B). In microhabitats such as cryoconite holes, where multiple organisms are in competition for organic carbon, it is necessary for some organisms to synthesize glucose from the acetate generated via fatty acid oxidation (Link et al., 2015). These fatty acids can be directed towards EPS production by autogenic ecosystem engineers such as filamentous cyanobacteria and for maintenance of cell membrane integrity, while other fatty acids, recognized as prominent stress-induced hormones in specific kingdoms, respond to temperature and UV-stress (Tsuji, 2016). These polyunsaturated fatty acids (PUFAs) have been found to trigger a respiratory burst in algal systems to control the growth of bacterial biofilms by limiting the action of degradative products (Küpper et al., 2009). Further processing of these of these PUFAs leads to the production of such as hydroperoxyeicosatetraenoic acid (5-HPETE; arachidonic acid 5-hydroperoxide) or the linolenic acid derivative, jasmonic acid. Both of these derivatives have been associated with responses to stress and were relatively lower in G4. Sn-glycerol-3-phosphate is central in components in glycerophospholipids (such as linolenic acid, linolenic acid, and arachidonic acid) but these seem to be diverted to the production of the saturated phospholipid, stearic acid (C18:0). This may be desaturated to form oleic acid (C18:1|) but levels of this metabolite were also lower in G4. The possible diversion from desaturation in G4 would not only reduce the levels of stress associated PUFA derivatives but will make membranes more rigid (Hąc-Wydro & Wydro, 2007). Membrane lipid unsaturation has been extensively linked to chilling tolerance (Edwards et al., 2020). While the temperatures of seasonally-open cryoconite holes are modulated by the flow of cold meltwater (Cook, Edwards, Takeuchi, & Irvine-Fynn, 2016) meaning temperature gradients within the cryoconite of different locations are unlikely, it may be that the earlier arrival of direct sunlight in morning on the easterly section of the ice cap results in the earlier displacement of diurnal freezing apparently in late season.

## Metabolomes reflect nitrogen assimilation and recycling

We observe a low-nitrogen environment where nutrient cycling due to microbiological action heavily influences the rates of nitrogen assimilation (Cameron et al., 2012). As nucleotides can also be indicators of nitrogen metabolism this could be an indication of greater nutrient cycling potential. However, other nitrogen indicators, amino acids and polyamines did correlate with nucleotide metabolite sectorial patterning (Figure 3D). In most biological systems, polyamines have been found to play a role in cell growth by protein synthesis enhancement, protein activity modulation, biofilm formation, and changes in membrane permeability (Zhu et al., 2015). Polyamines are aliphatic polycations that are present in all kingdoms, the most common of which are spermine (Spm), spermidine (Spd), putrecine (Put), cadaverine (Cad), 1,3 diaminopropane (Dap). In most biological systems, they have been found to play a role in cell growth and survival by protein synthesis enhancement, protein activity modulation, biofilm formation, and changes in membrane permeability (Krysenko & Wohlleben, 2022; Zhu et al., 2015). Metabolites are synthesized, catabolized and shunted by ABC (ATP binding cassette) transporters PotABCD (Spd) and PotFGHI (Put) and under acidic conditions PotE (Ornithine or Lysine/Put) and CadB (Lysine/Cad) according to the bacterial cell requirements. These metabolites are essential to transcription, translation, gene expression, regulation, autophagy and stress resistance (Miller-Fleming et al., 2015). Spermidine was shown to be involved in the maintenance of cell viability in cyanobacteria specifically under combined light and cold conditions, possibly through the promotion of transcription and/or translation by binding to nucleic acid targets (Igarashi & Kashiwagi, 2000; Zhu et al., 2015). Based on the degree of photosynthetic metabolite potential and high expression of specific TCA cycle metabolites, it is likely that these processes drive polyamine metabolism and N-assimilation in this localised region of the ice cap, highlighting the potential importance of polyamines as a cyanobacterial survival and nitrogen assimilation mechanism in this environment (Krysenko & Wohlleben, 2022; Zhu et al., 2015).

Previous studies of microbial growth under oligotrophic conditions have also provided evidence for the

observed class 1 glutamate, glutamate synthetase and class 2 amino acids preferring metabolically less-expensive pathways, that is, degradative pathways, to fulfil the cellular requirement for nucleotide biosynthesis (Link et al., 2015). This concept is additionally supported within this study by the presence of medium to high levels of xanthine and hypoxanthine alongside low levels of PRPP which confirm that salvaging is preferred over de novo synthesis of nitrogenous metabolites in the sampled ice cap cryoconite communities. It is likely this would prove energetically less demanding. Moreover, it would enable the demand for nitrogen-rich compounds to be met from recycling the limited pools of nitrogenous organic matter available (Barker et al., 2013), for example through necromass-associated organic matter liberated during lysis from the prolific levels of viral predation typical of glacier surfaces (Bellas et al., 2013). Indeed, polyamines such as those detected here have recently been implicated as 'danger signals' following the lytic discharge of polyamine-enriched intracellular milieu consequent to viral infection (de Mattos et al., 2023). Metagenomic analyses of cyanobacterial mats in other Arctic habitats highlight the importance of nutrient scavenging and recycling as an economical strategy for growth in the challenging prevailing conditions (Varin et al., 2010). Therefore, it is likely similar processes are pertinent in the metabolism of cryoconite communities within the High Arctic region.

## CONCLUSION

In this study, we use metabolomics to detail the functional elements of microbial ecosystems thriving at high elevations in the high Arctic. Ice cap surfaces represent some of the most austere terrestrial environments in the Northern hemisphere. Contemporary climatic warming is already profoundly apparent in its impact on glaciers and ice caps such as Foxfonna in central Svalbard (Geyman et al., 2022). The upper reaches of the Foxfonna ice cap investigated here reside at elevations well above the historical local equilibrium line altitude (ca. 621 m above sea level in 2007–8; (Rutter et al., 2011), which was the last year to show appreciable accumulation of ice mass). This has meant the seasonal window for the development of microbial communities upon its bare ice has been brief and annually variable. However, the extent and duration of bare ice exposure, and hence the most likely opportunity for cryoconite community development, is likely to continue expanding. Consequently, high plateau ice caps such as Foxfonna are likely to increase in their prominence as microbial habitats within the warming Arctic.

Within this study, metabolomics reveals cryoconite microbial communities of Foxfonna ice cap have biosynthetic pathways that can be linked to basic key metabolic functions for energy production and nutrient assimilation, with evidence that energy availability constrains the distribution of the functional groups in these cryoconite communities. There is an indication of the preferential use of metabolites generated by energetically cheaper pathways (i.e., degradative pathways) in order to sustain cellular growth in this environment as opposed to de novo synthesis, particularly in relation to nitrogen-containing metabolites. This study also suggests a prominent impact of East–West directional orientation that affects the metabolites present implying that organism function has a strong dependence on ice mass topography and light availability. Their ability to maintain biological functions under nutrient-poor, low temperature and acidic pH conditions results from microbial regulation of proteins, carotenoids and membrane lipids. Autotrophic processes in this environment are governed by photosynthetic taxa such as microalgae and cyanobacteria, including *Phormidesmis priestleyi*, a key member of the core community of this environment (Gokul et al., 2016), aiding provision of the necessary organic matter required for sustaining the heterotrophic members of the community and physical stability on ice cap surfaces.

## AUTHOR CONTRIBUTIONS

**Jarishma K. Gokul:** Formal analysis (lead); investigation (equal); methodology (equal); writing – original draft (equal). **Luis A. J. Mur:** Formal analysis (equal); methodology (equal); writing – original draft (equal). **Andrew J. Hodson:** Conceptualization (equal); investigation (equal); writing – review and editing (equal). **Tristram D. L. Irvine-Fynn:** Investigation (equal). **Aliyah R. Debbonaire:** Methodology (equal); writing – review and editing (equal). **Nozomu Takeuchi:** Investigation (equal); writing – review and editing (equal). **Arwyn Edwards:** Conceptualization (lead); data curation (equal); formal analysis (equal); funding acquisition (lead); investigation (equal); methodology (equal); project administration (lead); writing – original draft (equal); writing – review and editing (lead).

## ACKNOWLEDGEMENTS

We gratefully acknowledge the support of UNIS staff and students in sample collection and UKRI-NERC grants NE/S001034/1 and NE/V012991/1 to AE which support studies on Foxfonna, as well as Research Council of Norway BIOICE (288402) to AJH and AE. We are grateful for the Great Britain Sasakawa Foundation for supporting NT's fieldwork with TI-F and AE during sampling. Jarishma K. Gokul's PhD studies were supported by the South African National Research Foundation Study Abroad Scholarship (84991).

## CONFLICT OF INTEREST STATEMENT

No conflict of interest to declare.

## DATA AVAILABILITY STATEMENT

All data publicly available at DOI: 10.5281/zenodo.7669756.

## ORCID

*Arwyn Edwards* https://orcid.org/0000-0003-1762-8593

## REFERENCES


Anesio, A.M., Hodson, A.J., Fritz, A., Psenner, R. & Sattler, B. (2009) High microbial activity on glaciers: importance to the global carbon cycle. *Global Change Biology*, 15, 955–960.

Anesio, A.M. & Laybourn-Parry, J. (2012) Glaciers and ice sheets as a biome. *Trends in Ecology & Evolution*, 27, 219–225.

Barker, J., Dubnick, A., Lyons, W. & Chin, Y.-P. (2013) Changes in dissolved organic matter (DOM) fluorescence in proglacial Antarctic streams. *Arctic, Antarctic, and Alpine Research*, 45, 305–317.

Bellas, C., Anesio, A.M., Telling, J., Stibal, M., Tranter, M. & Davis, S. (2013) Viral impacts on bacterial communities in Arctic cryoconite. *Environmental Research Letters*, 8, 045021.

Bundy, J.G., Davey, M.P. & Viant, M.R. (2009) Environmental metabolomics: a critical review and future perspectives. *Metabolomics*, 5, 3–21.

Cameron, K., Hodson, A.J. & Osborn, A.M. (2012) Carbon and nitrogen biogeochemical cycling potentials of supraglacial cryoconite communities. *Polar Biology*, 35, 1375–1393.

Cameron, K.A., Stibal, M., Zarsky, J.D., Gözdereliler, E., Schostag, M. & Jacobsen, C.S. (2015) Supraglacial bacterial community structures vary across the Greenland ice sheet. *FEMS Microbiology Ecology*, 92, fiv164.

Cook, J., Edwards, A., Takeuchi, N. & Irvine-Fynn, T. (2016) Cryoconite: the dark biological secret of the cryosphere. *Progress in Physical Geography*, 40, 66–111.

Cook, J.M., Edwards, A., Bulling, M., Mur, L.A., Cook, S., Gokul, J.K. et al. (2016) Metabolome-mediated biocryomorphic evolution promotes carbon fixation in Greenlandic cryoconite holes. *Environmental Microbiology*, 18, 4674–4686.

de Mattos, C.D., Faith, D.R., Nemudryi, A.A., Schmidt, A.K., Bublitz, D.C., Hammond, L. et al. (2023) Polyamines and linear DNA mediate bacterial threat assessment of bacteriophage infection. *Proceedings of the National Academy of Sciences the United States of America*, 120, e2216430120.

Edwards, A., Cameron, K.A., Cook, J.M., Debbonaire, A.R., Furness, E., Hay, M.C. et al. (2020) Microbial genomics amidst the Arctic crisis. *Microbial Genomics*, 6, mgen000375.

Edwards, A., Debbonaire, A.R., Sattler, B., Mur, L.A., and Hodson, A.J. (2016) Extreme metagenomics using nanopore DNA sequencing: A field report from Svalbard, 78 N. bioRxiv 073965.

Edwards, A., Mur, L.A.J., Girdwood, S., Anesio, A., Stibal, M., Rassner, S.M. et al. (2014) Coupled cryoconite ecosystem structure-function relationships are revealed by comparing bacterial communities in alpine and Arctic glaciers. *FEMS Microbiology Ecology*, 89, 222–237.

Geyman, E.C., van Pelt, W.J.J., Maloof, A.C., Aas, H.F. & Kohler, J. (2022) Historical glacier change on Svalbard predicts doubling of mass loss by 2100. *Nature*, 601, 374–379.

Gokul, J.K., Cameron, K.A., Irvine-Fynn, T.D., Cook, J.M., Hubbard, A., Stibal, M. et al. (2019) Illuminating the dynamic rare biosphere of the Greenland ice sheet's dark zone. *FEMS Microbiology Ecology*, 95, fiz177.

Gokul, J.K., Hodson, A.J., Saetnan, E.R., Irvine-Fynn, T.D., Westall, P.J., Detheridge, A.P. et al. (2016) Taxon interactions control the distributions of cryoconite bacteria colonizing a high Arctic ice cap. *Molecular Ecology*, 25, 3752–3767.

Hąc-Wydro, K. & Wydro, P. (2007) The influence of fatty acids on model cholesterol/phospholipid membranes. *Chemistry and Physics of Lipids*, 150, 66–81.

Hodson, A., Anesio, A.M., Tranter, M., Fountain, A., Osborn, M., Priscu, J. et al. (2008) Glacial ecosystems. *Ecological Monographs*, 78, 41–67.

Hodson, A., Boggild, C., Hanna, E., Huybrechts, P., Langford, H., Cameron, K. et al. (2010) The cryoconite ecosystem on the Greenland ice sheet. *Annals of Glaciology*, 51, 123–129.

Hodson, A., Cameron, K., Bøggild, C., Irvine-Fynn, T., Langford, H., Pearce, D. et al. (2010) The structure, biogeochemistry and formation of cryoconite aggregates upon an Arctic valley glacier; Longyearbreen, Svalbard. *Journal of Glaciology*, 56, 349–362.

Igarashi, K. & Kashiwagi, K. (2000) Polyamines: mysterious modulators of cellular functions. *Biochemical and Biophysical Research Communications*, 271, 559–564.

Irvine-Fynn, T.D.L., Bridge, J.W. & Hodson, A.J. (2010) Rapid quantification of cryoconite: granule geometry and in situ supraglacial extents, using examples from Svalbard and Greenland. *Journal of Glaciology*, 56, 297–308.

Jarvis, R.M., Broadhurst, D., Johnson, H., O'Boyle, N.M. & Goodacre, R. (2006) PYCHEM: a multivariate analysis package for python. *Bioinformatics*, 22, 2565–2566.

Krysenko, S. & Wohlleben, W. (2022) Polyamine and ethanolamine metabolism in bacteria as an important component of nitrogen assimilation for survival and pathogenicity. *Medical Science*, 10, 40.

Küpper, F.C., Gaquerel, E., Cosse, A., Adas, F., Peters, A.F., Müller, D.G. et al. (2009) Free fatty acids and methyl jasmonate trigger defense reactions in *Laminaria digitata*. *Plant and Cell Physiology*, 50, 789–800.

Langford, H., Hodson, A., Banwart, S. & Bøggild, C. (2010) The microstructure and biogeochemistry of Arctic cryoconite granules. *Annals of Glaciology*, 51, 87–94.

Langford, H.J., Irvine-Fynn, T.D.L., Edwards, A., Banwart, S.A. & Hodson, A.J. (2014) A spatial investigation of the environmental controls over cryoconite aggregation on Longyearbreen glacier, Svalbard. *Biogeosciences*, 11, 5365–5380.

Lankadurai, B.P., Nagato, E.G. & Simpson, M.J. (2013) Environmental metabolomics: an emerging approach to study organism responses to environmental stressors. *Environmental Reviews*, 21, 180–205.

Link, H., Fuhrer, T., Gerosa, L., Zamboni, N. & Sauer, U. (2015) Real-time metabolome profiling of the metabolic switch between starvation and growth. *Nature Methods*, 12, 1091–1097.

Lutz, S., Anesio, A.M., Field, K. & Benning, L.G. (2015) Integrated 'omics', targeted metabolite and single-cell analyses of Arctic snow algae functionality and adaptability. *Frontiers in Microbiology*, 6, 1323.

Mahawar, L., Pandey, A., Ramasamy, K.P., Pandey, S. & Prasad, S.M. (2022) GABA as a signalling molecule: possible mechanism for its enhanced commercial production by cyanobacteria. *Journal of Applied Phycology*, 34, 2355–2369.

Miller-Fleming, L., Olin-Sandoval, V., Campbell, K. & Ralser, M. (2015) Remaining mysteries of molecular biology: the role of polyamines in the cell. *Journal of Molecular Biology*, 427, 3389–3406.

Müller, F. (1962) Zonation in the accumulation area of the glaciers of Axel Heiberg Island, NWT, Canada. *Journal of Glaciology*, 4, 302–311.

Murakami, T., Takeuchi, N., Mori, H., Hirose, Y., Edwards, A., Irvine-Fynn, T. et al. (2022) Metagenomics reveals global-scale contrasts in nitrogen cycling and cyanobacterial light-harvesting mechanisms in glacier cryoconite. *Microbiome*, 10, 1–14.

Noël, B., Jakobs, C.L., van Pelt, W., Lhermitte, S., Wouters, B., Kohler, J. et al. (2020) Low elevation of Svalbard glaciers drives high mass loss variability. *Nature Communications*, 11, 4597.

Ren, Z., Martyniuk, N., Oleksy, I.A., Swain, A. & Hotaling, S. (2019) Ecological stoichiometry of the mountain cryosphere. *Frontiers in Ecology and Evolution*, 7, 360.

Rutter, N., Hodson, A., Irvine-Fynn, T. & Solas, M.K. (2011) Hydrology and hydrochemistry of a deglaciating high-Arctic catchment, Svalbard. *Journal of Hydrology*, 410, 39–50.

Sawstrom, C., Laybourn-Parry, J., Mumford, P., Marshall, W. & Hodson, A. (2002) The microbial communities and primary productivity of cryoconite holes in an Arctic glacier (Svalbard 79 degrees N). *Polar Biology*, 25, 591–596.

Segawa, T., Yonezawa, T., Edwards, A., Akiyoshi, A., Tanaka, S., Uetake, J. et al. (2017) Biogeography of cryoconite forming cyanobacteria on polar and Asian glaciers. *Journal of Biogeography*, 44, 2849–2861.

Takeuchi, N. (2002) Optical characteristics of cryoconite (surface dust) on glaciers: The relationship between light absorency and the property of organic matter contained in the cryoconite. *Annals of Glaciology*, 34, 409–414.

Takeuchi, N., Kohshima, S., Goto-Azuma, K. & Koerner, R. (2001) Biological characteristics of dark colored material (cryoconite) on Canadian Arctic glaciers (Devon and penny ice caps). *Memoirs of the National Institute of Polar Research*, 54, 495–505.

Takeuchi, N., Kohshima, S. & Seko, K. (2001) Structure, formation, and darkening process of albedo-reducing material (cryoconite) on a Himalayan glacier: a granular algal mat growing on the glacier. *Arctic Antarctic and Alpine Research*, 33, 115–122.

Tranter, M., Fountain, A.G., Fritsen, C.H., Berry Lyons, W., Priscu, J.C., Statham, P.J. et al. (2004) Extreme hydrochemical conditions in natural microcosms entombed within Antarctic ice. *Hydrological Processes*, 18, 379–387.

Tsuji, M. (2016) Cold-stress responses in the Antarctic basidiomycetous yeast Mrakia blollopis. *Royal Society Open Science*, 3, 160106.

Uetake, J., Tanaka, S., Segawa, T., Takeuchi, N., Nagatsuka, N., Motoyama, H. et al. (2016) Microbial community variation in cryoconite granules on Qaanaaq glacier, NW Greenland. *FEMS Microbiology Ecology*, 92, fiw127.

Varin, T., Lovejoy, C., Jungblut, A.D., Vincent, W.F. & Corbeil, J. (2010) Metagenomic profiling of Arctic microbial mat communities as nutrient scavenging and recycling systems. *Limnology and Oceanography*, 55, 1901–1911.

Zhu, X., Li, Q., Yin, C., Fang, X. & Xu, X. (2015) Role of spermidine in overwintering of cyanobacteria. *Journal of Bacteriology*, 197, 2325–2334.

## SUPPORTING INFORMATION

Additional supporting information can be found online in the Supporting Information section at the end of this article.

**How to cite this article:** Gokul, J.K., Mur, L.A.J., Hodson, A.J., Irvine-Fynn, T.D.L., Debbonaire, A.R., Takeuchi, N. et al. (2023) Icescape-scale metabolomics reveals cyanobacterial and topographic control of the core metabolism of the cryoconite ecosystem of an Arctic ice cap. *Environmental Microbiology*, 1–15. Available from: https://doi.org/10.1111/1462-2920.16485